Indian Journal of Biochemistry & Biophysics
Vol. 61, August 2024, pp. 485-496
DOI: 10.56042/ijbb.v61i8.8515

Evaluation of inhibitory activity of few selected triazoles on xanthine oxidase – *In silico* studies

V Louwkhyaa[1], N Yogi Babu[2] & Deva Das Manwal[1]*

[1]Department of Chemistry, Osmania University, Hyderabad-500 007, Telangana, India

[2]Department of Chemistry, Dr. APJ Abdul Kalam Govt, Degree College, Patancheru, Sanga Reddy-502 319, Telangana State, India

Received 03 February 2024; *revised 02 April 2024*

Hyperuricemia, also called Gout is a medical term used for joints pain associated with increased levels of uric acid in blood serum of a patient. The end product of purine metabolism in human body is uric acid. An enzyme called Xanthine Oxidase (XO) is a catalyst for this purine metabolism. Inhibitor which reduces the activity of an enzyme is used as a therapeutic agent to maintain the desired levels of uric acid in blood serum of patients. Such available inhibitors in the market include Febuxostat and Allopurinol which are widely used by Rheumatologists. The search for new molecules which can act as better inhibitor than the inhibitors presently available in the market is never ending. Eighteen various triazole (5 newly designed) compounds have been identified and their inhibitory activity(*in silico*) is evaluated on Xanthine Oxidase and it is found that all these triazoles show much better inhibitory activity on said enzyme, when compared to Febuxostat and Allopurinol.

Keywords: Febuxostat, *In silico* Studies, Inhibitory activity, Selected triazoles, Uric acid, Xanthine Oxidase

Research is going on to find new strategies to prevent and treat a painful gout attacks. New drugs are being developed to maintain serum uric acid levels and reduce the pain. Febuxostat, Allopurinol and Topiroxostat are extensively used[1,2] by Rheumatologists to treat the patients suffering with Gout or hyperuricemia. It is a type of Arthritis commonly called as joint pain. In medical terminology, it is called hyperuricemia, means excess serum uric acid. It is characterized by sudden severe attacks of pain, swelling, redness and tenderness in one joint or in more joints. Gout usually attacks big toe, but it can appear in any joint. Other commonly affected joints include ankle, knees, elbows, wrists and fingers.

The main reason for Gout is increased serum uric acid levels in patients. Uric acid is a by-product of purine metabolism in human body. Untreated increased levels of uric acid would lead to crystallization (called Urates, hard and sharp needle like structures) and deposition of crystals in various parts of human body, *viz*, joints, kidneys and connecting tissues. The sharp crystals of uric acid which were deposited in joints, pierce into soft tissue and creates a wound in joints leading to inflammation with severe pain. Deposits in kidney are generally referred as kidney stones.

The uric acid has also proven to be harmful. The urate behaves as a pro-oxidant and induces the formation of other radicals that have a tendency to oxidize lipid membranes, which explains the correlation between hyperuricemia and obesity. Reactive oxygen species naturally tend to damage cellular structures, DNA, and proteins. and consequently, oxidative stress caused by uric acid also has links to hypertension, diabetes, kidney disease and cardiovascular diseases.

The reaction carried out by XO reduces oxygen into superoxide anion which eventually progresses into hydrogen peroxide. Hydrogen peroxide is a reactive oxygen species (ROS), the excess of which is toxic to individual cells. It also has links to aging and a multitude of conditions such as diabetes and neurodegenerative disorders such as Alzheimer disease[3].

Normally, uric acid dissolves in the blood and passes through kidneys in to urine. Sometimes, either body produces excessive uric acid or kidney excretes too low amount of uric acid, when this happens uric acid can build up in blood serum. Therefore, one can understand this problem under four headings i) *decreased excretion*; due to medicines like diuretics (thiazide), excessive alcohol reduces the excretion ii)

*Correspondence:
E-mail: ddmanwaall@gmail.com

over production: due to food (purine rich *e.g*., meat, seafood and sugar), due to liquids (beer, wine and sugar-coated liquids) iii) due to over activity of enzyme called 'Xanthine Oxidase'(XO) and iv) other[4] factors: oxidative stress is associated with increased activity of Xanthine Oxidase. This paper deals with controlling the over activity of xanthine oxidase.

The successful method of treating these conditions is to reduce the uric acid levels in blood serum to prevent the processes of crystallization. Out of four main areas mentioned above, the controlling the over activity of concerned enzyme by using inhibitors are most sought out options in these days.

Inhibitors attracted the attention of chemists and of late, they became the first choice as a target and they became a safe option compared to other available options to treat the Gout.

Allopurinol (analog of hypoxanthine) got US FDA approval in1966 as an effective inhibitor of Xanthine Oxidase. Later, it was realized that the active isomer, which effectively inhibits the XO is oxipurinol. This was considered as the *gold standard* inhibitor[5] for inhibition of Xanthine Oxidase and has been widely prescribed due to its excellent pharmacokinetics. However, it has half-life period of five hours, therefore high-dose prescription was inevitable which had drastic side effects. And there was a race to investigate more effective, long-lasting inhibitor for Xanthine Oxidase: and following are the winners in the race: BOF-4272, Febuxostat (2009), Topiroxostat (2013), which suffers with side effects in the form of fever, abdominal pain, skin rashes, allergic diarrhea and others which can damage liver, apart from positive outcome of reducing the serum uric acid. Due to the fact that commercialized drugs show side effects[6]; in recent years, large number of new alternative inhibitors were identified and tested for activity in *in vitro* studies, but majority of tested products do not advance for further pharmacological evaluation.

There is a significant amount of literature[7] available on natural products extracted from various plants, which demonstrate strong potential as inhibitors of XO activity.

Literature[8-16]survey also reveals that 1,2,3-triazole and 1,2,4-triazole moieties are the fundamental units favored in many drugs and their analogues have generated great deal of attention in the field of medicinal chemistry. Several papers[17-20] have been published exploring the inhibitory effects of triazoles on xanthine oxidase. These papers likely investigated the synthesis and biological evaluation of various triazole derivatives to assess their potency and selectivity as xanthine oxidase inhibitors.

In this backdrop, our study aims to identify new compounds that can efficiently inhibit the targeted enzyme while also possessing favorable pharmacokinetic properties. We seek to evaluate these potential inhibitors as alternatives to existing medications in the market, with the goal of minimizing side effects and improving overall therapeutic outcomes. As a part of strategy, we have first undertaken *in silico* studies[21-23] to find better molecule than what we have in the market, in the process we landed up in selecting 13 structures (Fig. 1A) known for their inhibitory activity. Along with known 13 structures, we generated 5 new alternate molecules (Fig. 1B) which are potential enough for the purpose along with 3 standard drugs (Fig. 1C) and conducted *in silico* studies. The results were compared with those of standard drugs and it is found that new molecules show better inhibiting activity.

Materials and Methods

Retrieval of the target protein structure

X- ray Crystal structure of Xanthine Oxidase retrieved from PDB ID IN5X[24], the structure was homodimer with chain A and B, only Chain A was used for further studies.

Preparation of protein

The protein was prepared and refined using Discovery Studio (DS) protein preparation module. First, the protein was imported into DS and cleaned using the clean Protein protocol, which removed ligands, cofactors, and water molecules from the crystal structure to get rid of false positive results and increase the accuracy of the results[25]. Then, hydrogen atoms were added, missing atoms and residues were replaced, amino acid atoms were rearranged, and terminal groups and ionizable side chains were protonated based on predicted pKa values. The structure was further improved and geometries optimized using the CHARMm force field and standard minimization procedures in DS. The minimization procedure consisted of 1000 maximal steps for both the conjugate gradient and steepest descent algorithms, each applied with a 0.1 Å RMS gradient, to achieve a stable and minimal energy conformation of the protein.

Ligand Generation and Optimization

Twenty-one compounds were used as ligands. Out of 21, 13 compounds that have been reported with

inhibition properties are selected and 3 ligands /drugs available in market were taken as reference ligands and remaining 5 compounds are newly generated. ACD/ChemSketch (12.0) was used for drawing the 2D structures of all aforesaid ligands and the resulted files were retained in mol.file format. DS protocols were maintained preparing the ligands through CHARMm force field application. CHARMm force field based energy minimization of the ligands proceed using a total of 1000 maximum steps at a root mean square gradient of 0.001°A till global minima have been attained to obtain lowest-energy ligand conformer.

A

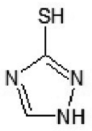

COMPOUND 1:
1H-1,2,4-triazole-3-thiol

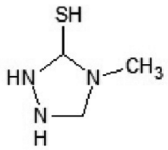

COMPOUND 2:
4-methyl-1,2,4-triazolidine-3-thiol

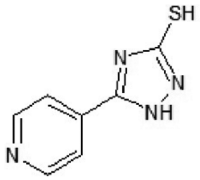

COMPOUND 3:
5-(pyridin-4-yl)-1H-1,2,4-triazole-3-thiol

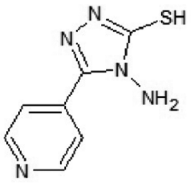

COMPOUND 4:
4-amino-5-(pyridin-4-yl)-4H-1,2,4-triazole-3-thiol

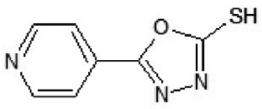

COMPOUND 5:
5-(pyridin-4-yl)-1,3, 4-oxadiazole-2-thiol

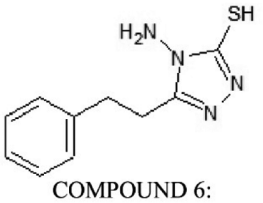

COMPOUND 6:
4-amino-5-(2-phenylethyl) -4H-1,2,4-triazole-3-thiol

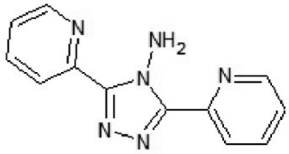

COMPOUND 7:
3,5-di(pyridin-2-yl)-4H-1,2,4-triazol-4-amine

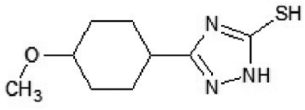

COMPOUND 8:
3-(4-methoxycyclohexyl)-1H-1,2,4-triazole-5-thiol

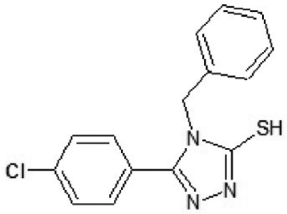

COMPOUND 9:
4-benzyl-5-(4-chlorophenyl)-4H-1,2,4-triazole-3-thiol

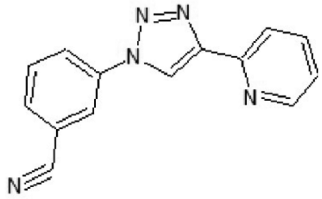

COMPOUND 10:
3-[4-(pyridin-2-yl)-1H-1,2,3- triazol-1-yl] benzonitrile

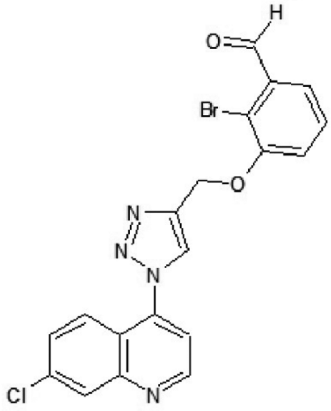

COMPOUND 11:
2-bromo-3-{[1-(7-chloroquinolin-4-yl)-1H-1,2,3-triazol-4-yl]methoxy}benzaldehyde

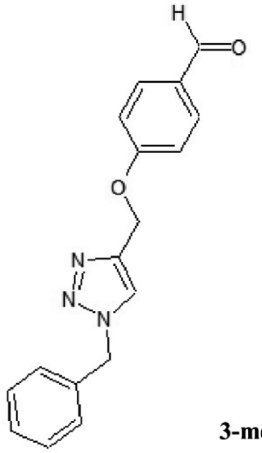

COMPOUND 12:
4-[(1-benzyl-1H-1,2,3-triazol-4-yl) methoxy] benzaldehyde

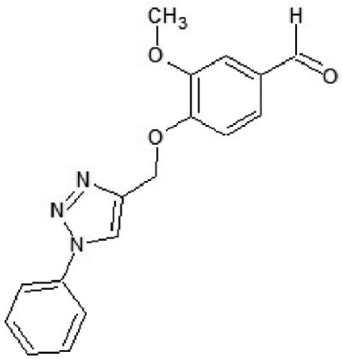

COMPOUND 13:
3-methoxy-4-[(1-phenyl-1H-1,2,3-triazol-4-yl) methoxy] benzaldehyde

Fig. 1A — Structures of ligands under study; Triazoles with known XO inhibition activity

B

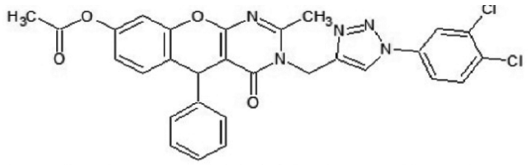

COMPOUND 14: **3-{[1-(3,4-Dichlorophenyl)-1H-1,2,3-triazol-4-yl] methyl}-2-methyl-4-oxo-10-phenyl-9-oxa-1,3-diaza-3,10-dihydro-4H-anthr-7-yl acetate**

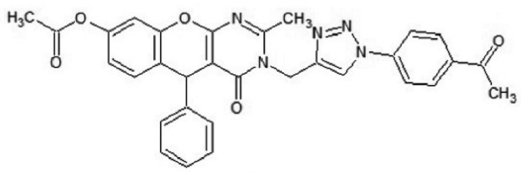

COMPOUND 15: **3-{[1-(p-Acetylphenyl)-1H-1,2,3-triazol-4-yl]methyl}-2-methyl-4-oxo-10-phenyl-9-oxa-1,3-diaza-3,10-dihydro-4H-anthr-7-yl acetate**

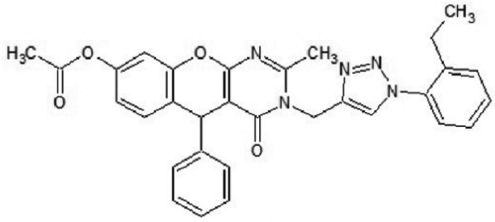

COMPOUND 16: **3-{[1-(o-Ethylphenyl)-1H-1,2,3-triazol-4-yl] methyl}-2-methyl-4-oxo-10-phenyl-9-oxa-1,3-diaza-3,10-dihydro-4H-anthr-7-yl acetate**

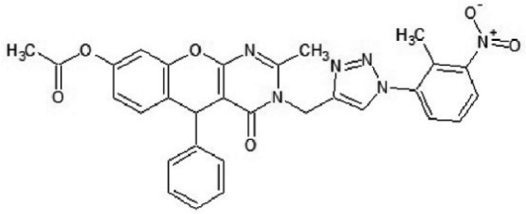

COMPOUND 17: **2-Methyl-3-{[1-(3-nitro-2-tolyl)-1H-1,2,3-triazol-4-yl] methyl}-4-oxo-10-phenyl-9-oxa-1,3-diaza-3,10-dihydro-4H-anthr-7-yl acetate**

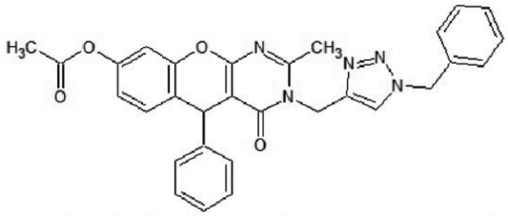

COMPOUND 18: **3-[(1-Benzyl-1H-1,2,3-triazol-4-yl)methyl]-2-methyl-4-oxo-10-phenyl-9-oxa-1,3-diaza-3,10-dihydro-4H-anthr-7-yl acetate**

Fig. 1B — Structures of ligands under study; Newly generated triazoles

Defining Binding Site

The active site of the XO was identified using the Define and Edit Binding Site tools in DS.

Molecular Docking

The Molecular Docking[26] studies were conducted using DS LibDock module. Ligands with high LibDock scores and lowest binding energy (protein – ligand interaction) was selected for optimal binding pose. Further the Analyse Ligand poses subprotocol in DS was utilized to assess all docking positions and the optimal position for each compound's binding interactions and was then examined. The outcome docking results were finally compared with reference drugs.

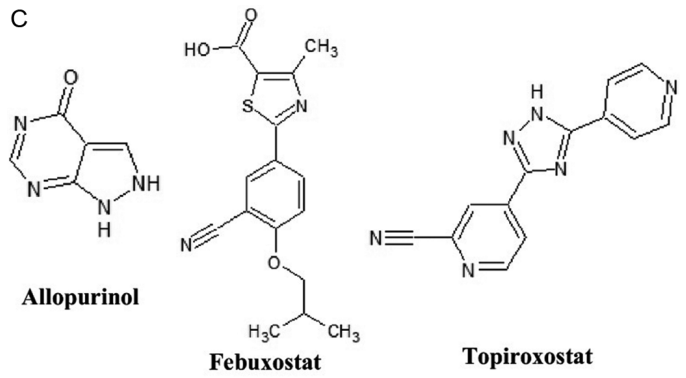

Fig. 1C — Structures of ligands under study; Available drugs in the market

Structure-based pharmacophore modeling

Using current knowledge of protein-ligand interactions, structure-based pharmacophore modeling[27] is employed to uncover crucial structural characteristics of the target protein, bovine XOD. This involves calculating potential interactions and their locations within the protein's active site using the DS "Interaction Generation" methodology. Subsequently, a pharmacophore query is generated *via* Ludi interaction maps to evaluate hydrophobic characteristics, hydrogen bond acceptors, and donors within the active site. After grouping selected features using the Edit and Cluster Pharmacophores tool, a structure-based pharmacophore model is formed with minimal and maximal features set to 1 and 2, respectively. This model is validated by considering compound orientation in the active region through the DS ligand pharmacophore mapping protocol, assessing the predictive capability based on best-fit values indicating compound mapping accuracy onto pharmacophoric attributes.

Molecular properties analysis

Drug-likeness is a molecular modeling technique applied to the development of drugs for identifying compounds that satisfy the Lipinski, Veber, Mueggue and Igan rules, these three crucial rules that must be met in order for a molecule to be submitted as a therapeutic candidate. It is a calibration for a drug's physicochemical properties with the pharmacokinetic properties in the human body. With the use of DS computer molecular properties approach, the drug-likeliness molecular characteristics of the compounds under study were determined by applying the five principles of Lipinski. Most of the active biological pharmaceuticals have a molecular weight less than 500, a log P (octanol/water coefficient) of less than 5, hydrogen bond donors of less than five and hydrogen bond acceptor of less than ten.

ADMET studies

Drug Absorption, Distribution, Metabolism, Excretion and Toxicity (ADMET) module is studied in DS for the chosen ligands. In order to determine the pharmacological characteristics and appropriate fitness for human administration, the results of ADMET plays a key role in drug design. With the help of DS modules, the parameters relating to mathematical predictive ADMET pharmacokinetics were obtained for these ligands include intestinal absorption, hepatotoxicity, plasma protein binding (PPB), blood brain barrier(BBB). aqueous solubility and CY2D6 binding. Additionally, the confidence ellipses were plotted using AlogP98 and PSA_2D.

Due to limitations of software, evaluation of findings relies on standard parameters. Standard analysis values, such as level0 for human intestinal absorption, level3 and level 4 for solubility, level 0 for non-inhibitory property with CYP450 D6, level 3 for BBB penetration and level 0 for non-toxicity have been eliminated to identify drug-likeliness of compounds.

Results

Molecular docking

The crystal structure of Xanthine oxidase from bovine with bound inhibitor TEI-6720(PDBID: IN5X) was selected as our protein target. A meticulous approach to molecule design focusing on fostering desired hydrogen bonding, van der waal's interactions, alongside ensuring the ligand's flexibility within the binding pocket, is essential for achieving favorable docking scores[28].The binding free energy was calculated to evaluate the enzyme protein's ability to bind to its substrate. Compounds exhibiting higher Dock scores and forming hydrogen bonds with key amino acids were identified as promising lead compounds for XO inhibition. Using the DS molecular docking approach with LibDock module,

the interaction between protein and all 21 ligands were studied using docking simulation. The obtained LibDock scores for all 21 ligands/compounds are listed in (Table 1) along with other parameters *viz* binding energies, H-bond count and H-interactions *etc*. all the poses were ranked according to the docked scores and the pose having the highest LibDock score[29] is taken into consideration. The ligand poses with high LibDock scores are prioritized for predicting the optimal ligand binding conformation

Table 1 — The compounds' docking scores (LibDockScores), an overview of the interacting amino acids, and the interacting atoms' bond lengths for the compounds into the Xanthine Dehydrogenase active site

Name	LibDock Score	H-BOND Count	H-bond interactions	Distance	Binding energy (kcal/mol)
Compound_1	47.431	2	Compound_1:H8 - B:GLU802:OE1	2.365000	-316.66627
			Compound_1:H8 - B:GLU802:OE2	2.360000	
Compound_2	55.471	2	Compound_2:H9 - B:GLU802:OE1	1.821000	-298.77414
			Compound_2:H9 - B:GLU802:OE2	2.368000	
			Compound_2:H15 - B:ARG880:HH21	1.404000	
Compound_3	55.471	2	B:ARG880:HH21 - Compound_3:N11	1.861000	-348.17891
			Compound_3:H13 - B:GLU802:OE1	2.387000	
			Compound_3:H16 - B:ARG880:HH21	1.802000	
			Compound_3:C9 - B:ARG880:HH21	2.008000	
Compound_4	76.963	1	B:ARG880:HH21 - Compound_4:N13	1.698000	-226.2064
Compound_5	81.162	1	B:ARG880:HH21 - Compound_5:O2	2.427000	-241.94647
Compound_6	91.279	4	B:ARG880:HH21 - Compound_6:N3	1.880000	-264.24608
			Compound_6:H16 - B:MOS4004:O1	1.933000	
			Compound_6:H17 - B:GLU802:OE1	2.339000	
			Compound_6:H17 - B:GLU802:OE2	2.405000	
			Compound_6:H20 - B:PHE1009:HD2	1.456000	
Compound_7	90.772	1	Compound_7:H19 - B:GLU802:OE1	2.032000	-27.5102
Compound_8	86.238	1	Compound_8:H15 - B:MOS4004:O1	1.640000	-195.31519
Compound_9	95.504	0			-253.40888
Compound_10	94.402	0			-150.72317
Compound_11	131.796	1	B:ASN768:HD22 - Compound_11:O27	2.346000	-181.42839
			Compound_11:H34 - B:VAL1011:HG21	1.580000	
			Compound_11:H39 - B:LYS771:HZ2	1.634000	
Compound_12	116.537	2	B:LYS771:HZ2 - Compound_12:O8	2.052000	-248.70386
			B:SER876:HN - Compound_12:N15	2.177000	
			B:LEU873:HD22 - Compound_12:H29	1.662000	
			B:ASN768:HD22 - Compound_12:C7	2.084000	
			B:ASN768:HD22 - Compound_12:H27	1.088000	
Compound_13	123.963	5	B:ASN768:HD22 - Compound_13:O15	2.388000	-297.60549
			B:LYS771:HZ2 - Compound_13:O15	2.430000	
			B:SER876:HN - Compound_13:N1	2.441000	
			B:SER876:HN - Compound_13:N3	2.477000	
			Compound_13:H28 - B:LEU648:HD11	1.820000	
Compound_14	167.826	4	B:ASN768:HD22 - Compound_14:O17	1.505000	-46.28257
			B:ASN768:HD22 - Compound_14:O19	2.342000	
			B:LYS771:HZ2 - Compound_14:O17	2.267000	
			B:LYS771:HZ2 - Compound_14:O19	2.204000	
			Compound_14:H41 - B:LEU873:HD21	1.316000	
			Compound_14:H41 - B:LEU873:CD2	1.859000	
			Compound_14:H41 - B:LEU873:HD22	1.730000	
			Compound_14:H56 - B:PHE1009:HD2	1.739000	
			Compound_14:C23 - B:LEU873:HD22	1.937000	
			Compound_14:H53 - B:LEU873:HD22	1.407000	
			Compound_14:H54 - B:LEU1014:HD11	1.772000	
			Compound_14:H55 - B:PHE914:CZ	2.090000	
			Compound_14:H55 - B:PHE914:HZ	1.278000	
			Compound_14:C18 - B:ASN768:HD22	2.131000	
			Compound_14:H56 - B:PHE1009:HD2	1.739000	
			Compound_14:C18 - B:LYS771:HZ2	1.989000	

(*Contd*.)

Table 1 — The compounds' docking scores (LibDockScores), an overview of the interacting amino acids, and the interacting atoms' bond lengths for the compounds into the Xanthine Dehydrogenase active site. (*Contd*.)

Name	LibDock Score	H-BOND Count	H-bond interactions	Distance	Binding energy (kcal/mol)
Compound_15	141.023	3	B:ASN768:HD22 - Compound_15:O17	2.497000	-181.58904
			B:LYS771:HZ1 - Compound_15:O19	2.348000	
			B:LYS771:HZ2 - Compound_15:O19	2.366000	
			Compound_15:C18 - B:LYS771:HZ2	2.122000	
			Compound_15:C25 - B:LEU873:HA	2.182000	
			Compound_15:C25 - B:LEU873:HD22	2.094000	
			Compound_15:C27 - B:LEU873:HA	1.931000	
			Compound_15:H52 - B:ASN768:HD22	1.724000	
			Compound_15:H56 - B:LEU873:HD22	1.587000	
Compound_16	153.37	1	B:ASN768:HD22 - Compound_16:O19	2.417000	-197.21761
Compound_17	137.927	6	B:ASN768:HD22 - Compound_17:O17	1.892000	575.01593
			B:ASN768:HD22 - Compound_17:O19	1.890000	
			B:LYS771:HZ2 - Compound_17:O17	2.318000	
			B:LYS771:HZ2 - Compound_17:O19	2.298000	
			B:SER876:HG - Compound_17:O21	2.367000	
			B:SER876:HG - Compound_17:N30	1.764000	
			Compound_17:H57 - B:PHE1009:HB2	1.429000	
Compound_18	168.433	4	B:ASN768:HD22 - Compound_18:O17	1.880000	-258.61393
			B:ASN768:HD22 - Compound_18:O19	2.003000	
			B:LYS771:HZ2 - Compound_18:O17	2.463000	
			B:SER876:HG - Compound_18:N30	2.164000	
			Compound_18:C3 - B:LEU1014:HD21	2.216000	
			Compound_18:O10 - B:LEU648:HD21	1.825000	
			Compound_18:C18 - B:ASN768:HD22	2.185000	
			Compound_18:C18 - B:LYS771:HZ2	2.190000	
			Compound_18:H50 - B:LEU1014:HD23	1.695000	
			Compound_18:H48 - B:LEU873:HA	1.697000	
			Compound_18:H46 - B:SER876:HN	1.438000	
Allopurinol	82.124	5	B:ARG880:HH21 - Allopurinol:O10	1.698000	-342.34267
			B:THR1010:HN - Allopurinol:O10	2.391000	
			B:THR1010:HG1 - Allopurinol:N5	2.392000	
			B:THR1010:HG1 - Allopurinol:O10	2.484000	
			Allopurinol:H14 - B:GLU802:OE1	1.645000	
Febuxostat	115.304	6	B:ASN768:HD21 - Febuxostat:N8	2.1390002.373	-363.2245
			B:ASN768:HD22 - Febuxostat:N8	000	
			B:ARG880:HH21 - Febuxostat:O21	2.028000	
			B:ARG880:HH21 - Febuxostat:O22	1.869000	
			B:THR1010:HN - Febuxostat:O21	1.850000	
			B:THR1010:HG1 - Febuxostat:O21	1.956000	
Topiroxostat	101.206	1	B:ARG880:HH21 - Topiroxostat:N5	1.527000	664.17765
			Topiroxostat:C6 - B:THR1010:HG1	2.173000	
			Topiroxostat:H22 - B:THR1010:HN	1.673000	
			Topiroxostat:H22 - B:THR1010:HG1	1.363000	

and estimating the binding energies of protein-ligand complexes, with the highest scoring poses being selected for further analysis of binding interactions[30].

Docking scores and binding energies

The perusal of the docking scores (Fig. 2A-D and Table 1) reveals that compound-18 is well located into the active site of protein with highest docking score (168.433) when compared to reference drugs, Febuxostat (115.304), Topiroxostat (101.206) and Allopurinol (82.124). The calculated binding energies for the compound-18 is (-258.61393 kcal/mol) was slightly higher than those found for the drugs Allopurinol (-342.34267 kcal/mol), Febuxostat (-363.2245 kcal/mol) whereas the drug Topiroxostat (664.17765 kcal/mol) has showed positive binding energy. Compounds with a high LibDock score suggest that they are more geometrically, energetically, and chemically compatible with reference compounds.

Hydrogen bonds between protein and ligands

The interaction of the compound 18 with the amino acid residues in the catalytic site is depicted in (Fig. 2). The interaction between the compound 18

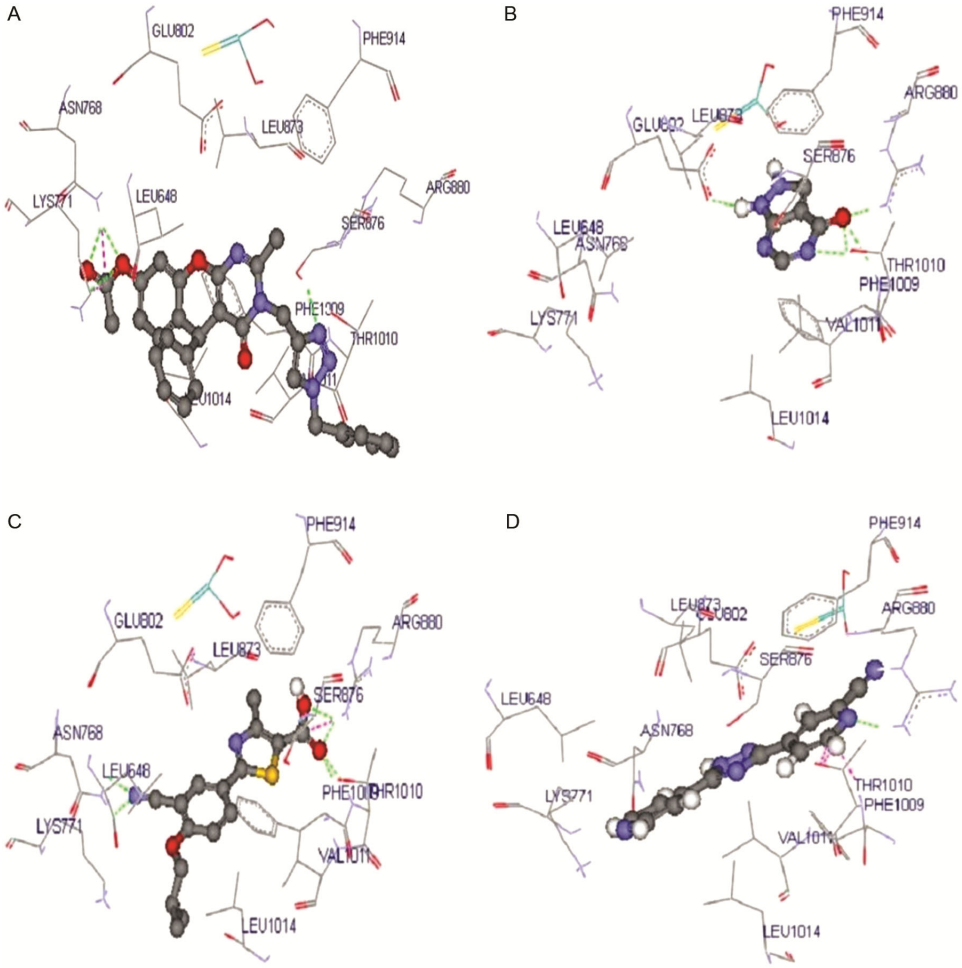

Fig. 2 — Computer generated interactions of XO with different compounds. (A) Interactions of XO with compound-18 (LibDock Score, 168.433); (B) Allopurinol (LibDock Score, 82.124); (C) Febuxostat (LibDock Score, 115.304); and (D) Topiroxostat (LibDock Score, 101.206)

and the XO catalytic site revealed that van der Waals interactions are predominant, although four hydrogen bonds were identified. The four hydrogen bonds are formed from the oxygen and nitrogen groups at O17 and O19 to ASN768 (B:ASN768:HD22 - Compound_18:O17 and B:ASN768:HD22 - Compound_18:O19) with a bond distance of 1.880000 Å and 2.003000 Å, O17 to LYS771(B:LYS771:HZ2 - Compound_18:O17) with a bond distance of 2.4630 Å and N30 to SER876(B:SER876:HG - Compound_18:N30) with a bond distance of 2.164 Å, respectively. The compound shows Vander Waals interactions with the carbon group at C3 and the hydrogen group at LEU1014 (Compound_18:C3 - B:LEU1014:HD21), oxygen at O10 and hydrogen at LEU648 (Compound_18:O10 - B:LEU648:HD21), carbon at C18 and hydrogen at ASN768 (Compound_18:C18 - B:ASN768:HD22), carbon C18 and hydrogen at LYS771 (Compound_18:C18 - B:LYS771:HZ2), carbon group at C18 and the hydrogen group at LEU1014 (Compound_18:H50 - B:LEU1014:HD23), carbon at C18 and alpha hydrogen at LEU873 (Compound_18:H48 - B:LEU873:HA) and carbon at C18 and hydrogen at SER876(Compound_18:H46 - B:SER876:HN) with a bond distances of 2.216000 Å, 1.825000 Å, 2.185000 Å, 2.190000 Å, 1.695000 Å, 1.697000 Å and 1.438000 Å.

Structure based pharmacophore modeling

Pharmacophore modeling complement molecular docking by aiding in the selection of drug leads with greater structural flexibility, while molecular docking provides a more precise calculation of specific binding interactions. Pharmacophore models can be developed *via* two methods: "structure-based" and "ligand-based" modeling. In the structure-based approach, the structural data of target proteins, like enzymes or receptors, is

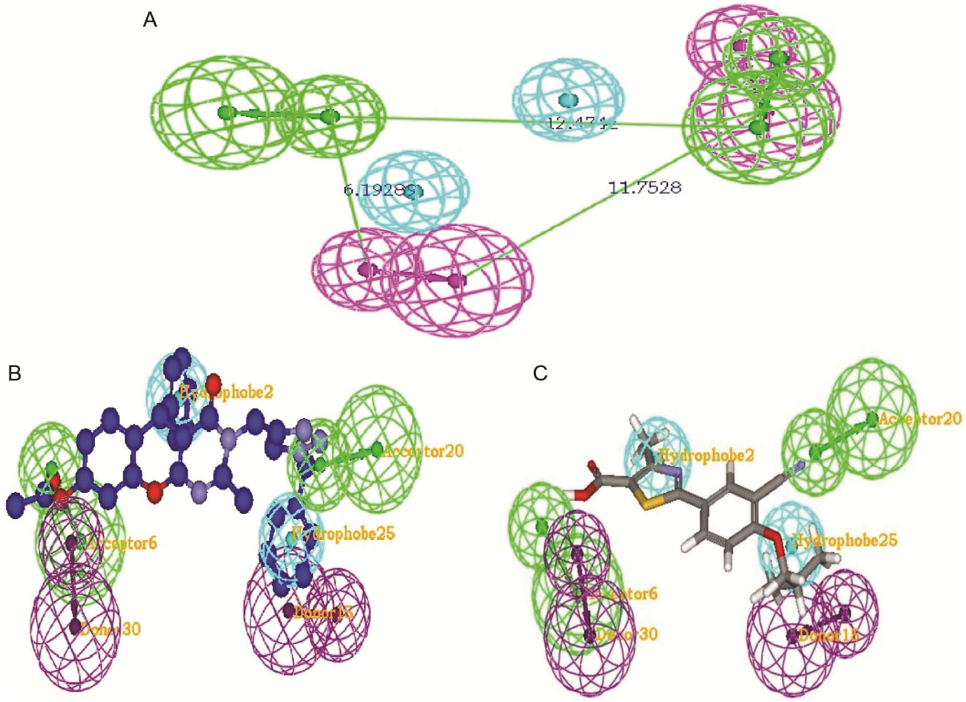

Fig. 3 — Structure based pharmacophore model. (A) Illustration of hydrophobic regions (light blue), the hydrogen bond acceptor (green) and the hydrogen bond donor (pink); (B) The compound 18 mapping the pharmacophore; and (C) Febuxostat mapping the pharmacophore

Table 2 — The fit values of the compounds

Name	Acceptor 20	Acceptor 6	Donor 15	Donor 30	Hydrophobe2	Hydrophobe25	Pharmprint	FitValue
Compound_17	1	1	0	0	1	1	'110011'	3.573
Compound_14	1	1	0	0	1	1	'110011'	3.297
Compound_15	1	1	0	0	1	1	'110011'	3.266
Compound_16	1	1	0	0	1	1	'110011'	3.129
Compound_18	1	1	0	0	1	1	'110011'	4.042
Compound_11	1	1	0	0	1	1	'110011'	2.669
Compound_13	1	1	0	0	1	1	'110011'	1.876
Febuxostat	1	1	0	0	1	1	'110011'	4.508

employed to identify potential drug compounds[31]. In this study, the structure-based pharmacophore method is adapted since the X-ray crystal structure of XO with bound inhibitor TEI-6720(PDB ID IN5X) is available in PDB. Interaction generation method of DS is used to calculate possible location of different interactions in active site of XO is evaluated. Subsequently, a pharmacophore query is generated through the Ludi interaction maps to evaluate the active site for hydrophobic characteristics, acceptors and donor sites of hydrogen bonds. Depending upon the best-fit values, which indicate how accurately the compounds have been mapped onto the pharmacophoric attributes, the predictive ability of the model was examined. Figure 3A illustrates the final edited pharmacophore model with two HBD, two HBA, and two hydrophobic characteristics. Compounds are mapped and ranked using ligand pharmacophore mapping in accordance with the fit values displayed in (Table 2). The predictive ability of the model was evaluated based on the best fit values, indicating the accuracy of compound mapping onto pharmacophoric features. Compounds were ranked by fit values, with higher values signifying better fit[32]. With a fit value of 4.04, as indicated in (Fig. 3B & C), compound 18 demonstrated good fitting on the pharmacophore.

Molecular properties analysis

The drug similarity and physicochemical properties are criteria for a new molecule to be judged in terms of a potential candidate for its biological activity. Many compounds show strong biological activity; nevertheless, due to their unfavorable qualities, they fail to be selected as pharmaceuticals. The famous Lipinski rule of five has been highly useful in this regard. For this reason, in this study, it is theoretically

verified whether our newly developed compounds satisfy criteria laid down by Lipinski *et al*[33], to be qualified as a drug. The Lipinski rule of five was applied to new compounds for evaluation and the different parameters obtained are listed in (Table 3). The rule of five says there should not be more than one violation of the following criteria: Hydrogen bonds should be < 5; Hydrogen acceptors should be < 10; Molecular mass should be < 500 Da and a calculated octane-water partition coefficient (Alog P) should be < 5; rotatable bonds should be < 10 and polar surface area should not be more than 140 $^0A^2$ (note: all the numbers are multiples of five, which is the origin of the rule name).

Discussion

The perusal of the values from Table 3 reveals that new compounds, except compounds-14 and 16, all showed their AlogP values less than 5, suggesting appropriate solubility in lipid and aqueous solutions, which is in line with the rule. The molar mass values of newly synthesized compounds under study are all marginally greater than 500 Da (deviation from rule five) and other compounds are less than 500Da suggesting their ability to pass through cellular membranes[34]. The values for H-acceptors and rotatable bonds are less than 10 for all the compounds under study and the vales for H-donors for all the compounds are less than 5, are in good agreement with the rule of five. Number of rings and aromatic rings less than 7 met the requirements of Muegge rule. The potential compound-18, has deviated in terms of molar mass (519.551) and qualified in all other parameters to be qualified as a drug through Lipinski test. The famous rule of five has been highly influential in this regard, but only about 50% of orally administered chemical entities actually obey it.

ADMET studies

Poor ADMET property is one of the main reasons for the failures during the drug development and clinical trials. Therefore, it is necessary to determine ADMET property[35] at this stage to avoid further failures in the pathway to develop new novel drugs. Hence compounds are subjects to additional scrutiny through pharmacokinetics and toxicity tests, employing the ADMET descriptors analysis technique in Discovery Studio. The parameters determined were presented in (Table 4). The results revealed that the compounds under study have low or indefinable values for blood brain barrier (BBB) penetration level (level 3 and 4) similar to reference drugs. Additionally, ninety-nine percent of the compounds displayed an absorption level of 0 and 1 suggesting favorable human intestinal absorption, except for compounds 14 and 17 which showed low absorption. The majority of compounds demonstrated ADME aqueous solubility levels between 2 and 3, indicating good aqueous solubility. The crucial property, Polar Surface Area (PSA), was associated with drug bioavailability[36]. Molecules with passive absorption and PSA < 140 were predicted to have lower bioavailability. Consequently, all synthesized compounds were anticipated to exhibit good passive oral

Table 3 — Molecular properties of the compounds

Name	ALogP	Molecular Weight	H_Acceptors	H_Donors	Rotatable Bonds	Rings	Aromatic Rings
Allopurinol	-1.479	136.111	5	2	0	2	0
Compound_1	0.47	101.13	3	2	0	1	1
Compound_10	2.692	247.255	4	0	2	3	3
Compound_11	4.729	443.681	5	0	5	4	4
Compound_12	3.137	293.32	4	0	6	3	3
Compound_13	3.114	309.319	5	0	6	3	3
Compound_14	5.743	574.414	7	0	6	6	4
Compound_15	4.154	547.561	8	0	7	6	4
Compound_16	5.357	533.577	7	0	7	6	4
Compound_17	4.795	564.548	9	0	7	6	4
Compound_18	4.421	519.551	7	0	7	6	4
Compound_2	0.366	119.189	4	3	0	1	0
Compound_3	1.245	178.214	4	2	1	2	2
Compound_4	0.378	193.229	5	2	1	2	2
Compound_5	0.88	179.199	4	1	1	2	2
Compound_6	2.019	220.294	4	2	3	2	2
Compound_7	1.107	238.248	5	1	2	3	3
Compound_8	1.745	213.3	4	2	2	2	1
Compound_9	4.474	301.794	3	1	3	3	3
Febuxostat	3.468	316.375	5	1	5	2	2
Topiroxostat	1.141	248.243	5	1	2	3	3

Table 4 — Predicted ADMET properties of the compounds

Name	BBB Level	Absorption Level	Solubility Level	Hepatotoxicity	CYP2D6	PPB Level	AlogP98	PSA_2D
Allopurinol	3	1	4	0	0	0	-1.091	65.567
Compound_1	3	0	4	1	0	0	0.47	37.577
Compound_10	2	0	3	1	1	2	2.692	62.066
Compound_11	1	0	1	1	1	2	4.729	65.362
Compound_12	2	0	3	1	1	2	3.137	54.101
Compound_13	2	0	3	1	1	2	3.114	63.031
Compound_14	4	2	1	1	1	2	5.743	95.007
Compound_15	4	1	2	1	1	2	4.154	112.308
Compound_16	4	1	1	1	1	2	5.357	95.007
Compound_17	4	2	2	1	1	2	4.795	137.83
Compound_18	4	0	2	1	1	2	4.421	95.007
Compound_2	2	0	4	0	0	0	1.143	28.972
Compound_3	3	0	3	1	0	0	1.245	48.838
Compound_4	3	0	3	1	0	0	0.378	65.671
Compound_5	3	0	4	1	0	2	0.88	46.337
Compound_6	2	0	3	1	0	2	2.019	54.41
Compound_7	3	0	3	1	1	2	1.108	76.932
Compound_8	2	0	3	1	0	0	1.745	46.507
Compound_9	0	0	2	1	1	2	4.474	27.87
Febuxostat	2	0	2	0	0	1	3.514	81.242
Topiroxostat	3	0	3	1	1	0	1.141	83.034

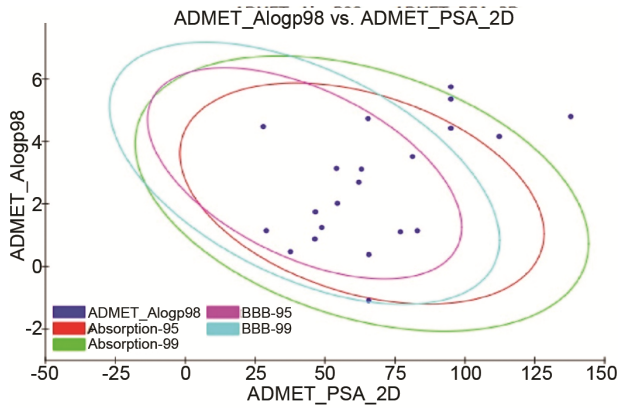

Fig. 4 — The plot of polar surface area and A Log P for the compounds

absorption[37]. The results were visualized in a 2D ADMET plot shown in (Fig 4), depicting the relationship between calculated PSA_2D with its corresponding computed atom-type partition coefficient (ALogP98) which yields the ADMET Descriptors. The ellipses represent the intestine absorption model and the BBB absorption model at 95% confidence limits.

Conclusion

This publication involves pharmacophore modeling and molecular docking studies to determine the structures of potential drugs and their inhibitory activity on Xanthine Oxidase. These compounds exhibited the lowest binding energy and higher docking score which were further refined using LibDock score and the corresponding interactions were determined. While fitting the compounds to the produced pharmacophore, the most appropriate hypothesis was used. Subsequently, the compounds' pharmacokinetics also has been investigated using ADMET and drug- likelihood studies. The results of this investigation would shed important light on the therapeutic potential of these compounds and emphasize the necessary for additional research investigations exploring the application of the newly designed triazole compounds as XO inhibitors.

Acknowledgement

The authors thank the HoD, Department of chemistry, Osmania University for moral support and encouragement and also providing necessary research facilities.

Conflicts of interest

All authors declare no conflict of interest**.**

References

1 Frampton JE, Febuxostat - A review of its use in the treatment of hyperuricemia in patients with gout. *Drugs*, 75 (2015) 427.

2 Chandrashekara S & Paul BJ, A narrative review of clinical evidence validating the efficacy of topiroxostat in managing hyperuricemia. *Indian J Rheumatol*, 17 (2022) 396.

3 Liu N, Xu H, Sun Q, Yu X, Chen W, Wei H, Jiang J, Xu Y & Lu W, The role of oxidative stress in hyperuricemia and xanthine oxidoreductase (XOR) inhibitors. *Oxid Med Cell Longev*, (2021) 1470380.

4 Nesari V, Vaishnav J, Sharma S, Nongthomba U & Balakrishnan S; Mitigation of pathological parameters under Jagged1 influence in DMD knockout zebrafish and patient-derived myoblast cultures. *Indian J Biochem Biophys,* 60 (2023) 681.

5 Massy V, Komai H, Palmer G & Elion GB, On the mechanism of inactivation of xanthine Oxidase by

allopurinol and other pyrazolo[3,4] pyrimidines. *J Bio Chem*, 245 (1970) 2837.
6 Anis TR & Meher J, Allopurinol-Induced Stevens–Johnson Syndrome (SJS). *Clin Pharmacol: Adv Appl,* (2023) 99.
7 Shalini Kapoor Mehta & Naira Nayeem, Natural Xanthine Oxidase inhibitors for Management of Gout: *A review*. *Res Rev J Med Health Sci,* 3 (2014) 1.
8 Ebenezer Oluwakemi, Jordaan MA, Carena G, Bono T, Shapi M & Tuszynski JA, An overview of the biological evolution of selected nitrogen-containing heterocyclic medicinal chemistry compounds. *Int J Mol Sci*, 23 (2022) 8117.
9 Rullo R, Cerchia C, Nasso R, Romanelli V, Vendittis ED, Massullo M & Lavecchia A, Novel reversible inhibitors of xanthine oxidase targeting the active site of the enzyme. *Antioxidants*, 12 (2023) 825.
10 Kotozaki Y, Satoh M, Nasu T, Tanno K, Tanaka F & Sasaki M, Human plasma xanthine oxidoreductase activity in cardiovascular disease: Evidence from a population –based study. *Biomedicines*, 11 (2023) 754.
11 Kumar S, Khokra SL & Yadav A, Triazole analogues as potential pharmacological agents: A brief review. *Future J Pharm Sci,* 7 (2021) 106.
12 Kumari M, Tahlan S, Narasimhan B, Ramasamy K, Lim SM, Shah SAA, Mani V & Kakkar S, Synthesis and biological evaluation of heterocyclic 1, 2, 4-triazole scaffolds as promising pharmacological agents. *BMC Chem*, 15 (2021) 1.
13 Juríček M, Kouwer PH & Rowan AE, Triazole: A unique building block for the construction of functional materials. *Chem Commun,* 47 (2011) 8740.
14 Matin MM, Matin P, Rahman MR, Ben Hadda T, Almalki FA, Mahmud S, Ghoneim, MM, Alruwaily M & Alshehri S, Triazoles and their derivatives: Chemistry, synthesis, and therapeutic applications. *Front Mol Biosci*, 9 (2022) 864286.
15 Vala DP, Vala RM & Patel HM, Versatile Synthetic Platform for 1, 2, 3-Triazole Chemistry. *ACS Omega*, 7 (2022) 36945.
16 Guo HY, Chen ZA, Shen QK & Quan ZS, Application of triazoles in the structural modification of natural products. *J Enzyme Inhib Med Chem*, 36 (2021) 1115.
17 Sato T, Ashizawa N, Iwanaga T, Nakamura H, Matsumoto K, Inoue T & Nagata O, Design, synthesis, and pharmacological and pharmacokinetic evaluation of 3-phenyl-5-pyridyl-1,2,4-triazole derivatives as xanthine oxidoreductase inhibitors. *Bioorg Med Chem Lett*, 19 (2009) 184.
18 Li SY, Zhang TJ, Wu QX, Olounfeh KM, Zhang Y & Meng FH, Synthesis and Biological Evaluation of 5-benzyl-3-pyridyl-1H-1,2,4-triazole Derivatives as Xanthine Oxidase Inhibitors. *Med Chem*, 16 (2020) 119.
19 Yang Y, Yan D, Cheng H, Nan G, Hou X, Ren L, Yang Y, Li X, Tian J, Ye F & Xiao Z, Discovery of novel 1,2,4-triazole derivatives as xanthine oxidoreductase inhibitors with hypouricemic effects. *Bioorg Chem*, 129 (2022) 1061.
20 Luna G, Dolzhenko AV & Mancera RL, Inhibitors of Xanthine Oxidase: Scaffold Diversity and Structure-Based Drug Design. *Chem Med Chem,* 14 (2019) 714.
21 Nalban N, Wanjari M, Matte S, Jamadagni P & Tamboli M, A comprehensive computational study of Millets derived phytochemicals as potential inhibitors of NACHT domain of NLRP3 inflammasome: Molecular docking, molecular dynamics simulation, MM-PBSA free energy calculation and DFT analysis. *Indian J Biochem Biophys,* 61 (2024) 223.
22 Latha V, Gomathi V, Rajeshkanna A & Hari Ram S, Generating a potent inhibitor against MCF7 breast cancer cell through artificial intelligence based virtual screening and molecular docking studies. *Indian J Biochem Biophys,* 60 (2023) 844.
23 Katiyar K, Srivastava RK, Nath R & Singh G, Cryptosporidiosis- a public health challenge: A combined 3D shape-based virtual screening, docking study, and molecular dynamics simulation approach to identify inhibitors with novel scaffolds for the treatment of cryptosporidiosis. *Indian J Biochem Biophys*, 59 (2022) 296.
24 Okamoto K, Eger BT, Nishino T, Kondo S, Pai EF & Nishino T, An extremely potent inhibitor of xanthine oxidoreductase: Crystal structure of the enzyme-inhibitor complex and mechanism of inhibition. *J Biol Chem*, 278 (2003) 1848.
25 Darji S, Trivedi P, Mehta V & Banerjee D, The role of water molecules and its dynamics to the binding site of β-lactamase enzyme with respect to β-lactamase inhibitor. *Indian J Biochem Biophys,* 60 (2023) 750.
26 Meng XY, Zhang HX, Mezei M & Cui M, Molecular Docking: A powerful approach for structure-based drug discovery. *Curr Comput Aided Drug Des*, 7 (2011) 146.
27 Gaurav A & Gautam V, Structure-based three-dimensional pharmacophores as an alternative to traditional methodologies. *J Receptor Ligand Channel Res,* 7 *(*2014) 27.
28 Rani KU, Sharma GVM, Saxena S, Guruprasad L & Padmavathi DA, Synthesis, DFT and Molecular docking study of novel bis 1,2,3-triazole derivatives of 2-hydroxyquinoline-4-carboxylate as antimicrobial agents. *Indian J Biochem Biophys*, 60 (2023) 729.
29 Alam S & Khan F, Virtual screening, Docking, ADMET and System Pharmacology studies on Garcinia caged Xanthone derivatives for Anticancer activity. *Sci Rep*, 8 (2018) 5524.
30 Hussain S, Chandrasekharan G, Komal KP & Sreenivasa E, Molecular docking analysis of doronine derivaties with human COX-2. *Biomed Inform*, 16 (2000) 483.
31 Baby ST, Sharma S, Enaganti S & Cherian PR, Molecular docking and pharmacophore studies of heterocyclic compounds as Heat shock protein 90 (Hsp90) Inhibitors. *Bioinformation*, 15 (2016) 149.
32 Giordano D, Biancaniello C, Argenio MA & Facchiano A, Drug Design by Pharmacophore and Virtual Screening Approach. *Pharmaceuticals (Basel)*, 23 (2022) 646.
33 Lipinski CA, Drug-like properties and the causes of poor solubility and poor permeability. *J Pharm Toxicol Methods,* 44 (2000) 235.
34 Erdogan T, Computational evaluation of 2-arylbenzofurans for their potential use against SARS-CoV-2: A DFT, molecular docking, molecular dynamics simulation study. *Indian J Biochem Biophys*, 59 (2022) 59.
35 Herri T, Thanmayalaxmi D & Suvitha A, ADMET, Pharmacokinetic and Docking properties of the fungal drug 2- (2, 4-difluorophenyl)-1, 3-bis (1, 2, 4-triazol-1-yl) propan-2-ol by using Quantum Computational Methods. *Indian J Biochem Biophys,* 60 (2023) 58.
36 Egan WJ, Merz KM & Baldwin JJ, Prediction of Drug Absorption Using Multivariate Statistics. *J Med Chem*, 43 (2000) 3867.
37 El-sattar NEAA, Badawy EHK, Abdel-Hady WH, Abo-Alkasem MI, Mandour AA & Ismail NSM, Design and Synthesis of New CDK2 Inhibitors Containing Thiazolone and Thiazolthione Scaffold with Apoptotic Activity. *Chem Pharm Bull,* 69 (2021) 106.